

Article

Antibacterial and Analgesic Properties of Beta-Caryophyllene in a Murine Urinary Tract Infection Model

Kayle Dickson ¹, Cassidy Scott ² , Hannah White ², Juan Zhou ³, Melanie Kelly ² and Christian Lehmann ^{1,2,3,4,*} ¹ Department of Microbiology and Immunology, Dalhousie University, Halifax, NS B3H 4R2, Canada² Department of Pharmacology, Dalhousie University, Halifax, NS B3H 4R2, Canada; cassidy.scott@dal.ca (C.S.); hannahwhite@dal.ca (H.W.)³ Department of Anesthesiology, Pain Management and Perioperative Medicine, Dalhousie University, Halifax, NS B3H 4R2, Canada; juan.zhou@dal.ca⁴ Department of Physiology and Biophysics, Dalhousie University, Halifax, NS B3H 4R2, Canada

* Correspondence: chlehmann@dal.ca

Abstract: Beta-caryophyllene has demonstrated anti-inflammatory effects in a variety of conditions, including interstitial cystitis. These effects are mediated primarily via the activation of the cannabinoid type 2 receptor. Additional antibacterial properties have recently been suggested, leading to our investigation of the effects of beta-caryophyllene in a murine model of urinary tract infection (UTI). Female BALB/c mice were intravesically inoculated with uropathogenic *Escherichia coli* CFT073. The mice received either beta-caryophyllene, antibiotic treatment using fosfomycin, or combination therapy. After 6, 24, or 72 h, the mice were evaluated for bacterial burden in the bladder and changes in pain and behavioral responses using von Frey esthesiometry. In the 24 h model, the anti-inflammatory effects of beta-caryophyllene were also assessed using intravital microscopy. The mice established a robust UTI by 24 h. Altered behavioral responses persisted 72 h post infection. Treatment with beta-caryophyllene resulted in a significant reduction in the bacterial burden in urine and bladder tissues 24 h post UTI induction and significant improvements in behavioral responses and intravital microscopy parameters, representing reduced inflammation in the bladder. This study demonstrates the utility of beta-caryophyllene as a new adjunct therapy for the management of UTI.

Keywords: cannabis; terpenes; pain; inflammation; intravital microscopy

Citation: Dickson, K.; Scott, C.; White, H.; Zhou, J.; Kelly, M.; Lehmann, C. Antibacterial and Analgesic Properties of Beta-Caryophyllene in a Murine Urinary Tract Infection Model. *Molecules* **2023**, *28*, 4144. <https://doi.org/10.3390/molecules28104144>

Academic Editor: David Barker

Received: 21 March 2023

Revised: 5 May 2023

Accepted: 15 May 2023

Published: 17 May 2023



Copyright: © 2023 by the authors. Licensee MDPI, Basel, Switzerland. This article is an open access article distributed under the terms and conditions of the Creative Commons Attribution (CC BY) license (<https://creativecommons.org/licenses/by/4.0/>).

1. Introduction

Urinary tract infections (UTIs) are a common type of infection involving the urethra, bladder, and/or kidneys which affect more than 400 million people annually [1,2]. Premenopausal females are disproportionately affected, experiencing UTIs 40 times as frequently as males of the same age [3]. Symptoms of a UTI affecting the lower tract (i.e., bladder) include increased urinary frequency, increased urinary urgency, pain, and blood in the urine. While not generally life-threatening, UTI symptoms are uncomfortable and decrease overall quality of life. If left untreated, lower UTIs may spread into the kidneys, resulting in systemic symptoms including fever and flank pain. Further progression of infection may result in serious sequelae, including sepsis and death. While most infections are not life-threatening and resolve with antibiotic therapy, UTIs cost the healthcare system billions of dollars each year [1]. This high cost is due in part to the high incidence of UTIs, but recurrent infections also play an important role. The rate of recurrence of infection within six months exceeds 25% despite adequate management with antibiotics [4].

UTIs are typically treatable with antibiotic therapy, including first-line treatments such as fosfomycin, nitrofurantoin, and trimethoprim/sulfamethoxazole (TMP/SMX) [5]. Other treatments, including fluoroquinolones, are available but have more significant side effects than first-line treatments [6]. However, the rates of bacterial resistance to antibiotics are rising, potentially limiting treatment options in the future [7]. Many species of bacteria that

commonly cause UTIs, including *Escherichia coli*, have shown resistance to multiple common antibiotic treatments. For example, the rates of resistance to TMP/SMX exceed 20% in some regions, preventing their use [8]. Nitrofurantoin and fosfomycin exhibit lower rates of resistance [9]. Increasing rates of multi-drug resistant UTI pathogens makes treatment more challenging and are especially concerning considering antibiotics are currently the only approved treatment for a UTI [10].

In addition to issues surrounding mounting resistance, antibiotic use frequently comes with unwanted side effects. Antibiotics can cause disturbances to the body's normal microbiome, specifically in the genitourinary and gastrointestinal tracts. These disturbances can result in candidiasis, which requires additional antimycotic therapy to resolve [11]. Antibiotics also take time to fully resolve the infection, meaning that symptoms of pain and discomfort can linger even after treatment has begun. Colgan and Williams noted that patients only begin to experience relief from UTI symptoms after 36 h [12]. Patients may need to take additional medications to manage these symptoms. Taken together with the threat of antibiotic resistance, these findings illustrate the need for additional, non-antibiotic-based strategies for the management of UTIs.

One strategy of interest for the management of this painful inflammatory condition is the modulation of the endocannabinoid system (ECS). The ECS plays an important role in the maintenance of physiological homeostasis, with a variety of effects across the entire body [13,14]. Major receptors in the system include the G-protein-coupled receptors cannabinoid type 1 receptor (CB₁R) and cannabinoid type 2 receptor (CB₂R) [13]. CB₁R agonism has anti-inflammatory and anti-nociceptive effects, but its prominence within the central nervous system (CNS) also results in psychoactive effects that make it an undesirable target for pain relief. In contrast, CB₂R is primarily found outside of the CNS, and receptor activation does not produce psychoactive effects. Within the bladder, CB₂R is expressed in the both the mucosa and the detrusor and is known to be upregulated in response to inflammation [15,16]. We have recently demonstrated the beneficial effects of CB₂R activation by the agonist beta-caryophyllene (beta-C) in a murine model of interstitial cystitis [17]. While interstitial cystitis is not infectious by definition, there is significant overlap between the symptoms of interstitial cystitis and UTI, with both conditions resulting in significant pain and inflammation.

Beta-C is a non-psychoactive sesquiterpene that occurs naturally in a variety of plants, including cannabis, cloves, and black pepper [18]. A recent systematic review of the literature identified a beta-C content $\geq 10\%$ in approximately 300 species across 51 different families [19]. Beta-C content reaches approximately 60% in certain species of fir tree (*Abies*) [20]. Beta-C is generally recognized as safe (GRAS), meaning that experts have deemed it safe for human consumption as it has a favorable toxicological profile [21]. While not a classical cannabinoid compound, beta-C acts through the endocannabinoid system by selectively and specifically binding CB₂R to produce anti-inflammatory effects [22]. In addition to its CB₂R-mediated effects, beta-C also exerts local anesthetic effects [23]. Its anti-bacterial activity has also been identified. Beta-C has shown anti-bacterial activity against multiple species of bacteria, including *E. coli* [22,23]. When taken in combination with the anti-inflammatory and associated with CB₂R agonism, these findings indicate that beta-C may represent a valuable addition to traditional antibiotic-based strategies for managing UTIs. As such, this study aims to investigate the effects of beta-C treatment in a murine model of UTI.

2. Results

We observed a significant but variable increase in the urinary bacterial burden six hours post inoculation (Figure 1A) which was not significantly reduced by co-treatment with beta-C, fosfomycin, or combination therapy. In subsequent experiments, additional urinary samples were collected six hours post inoculation, just prior to treatment with beta-C to minimize the variability observed in preliminary work. The animals were followed for 24 and 72 h to monitor the progress of infection. The urinary bacterial burden remained

high 24 h post inoculation and typically resolved by 72 h regardless of treatment status (Figure 1B,C). After 24 h, beta-C treatment resulted in a significant reduction in urinary bacterial burden (Figure 1A). There was no significant difference between treatment with 100 mg/kg beta-C and a low dose of fosfomycin (10 mg/kg), and no additional benefit from combination therapy was identified with respect to the bacterial burden. The anti-bacterial effects of beta-C were not abrogated by a blockade of the CB₂R with antagonist AM630 (Figure 1B).

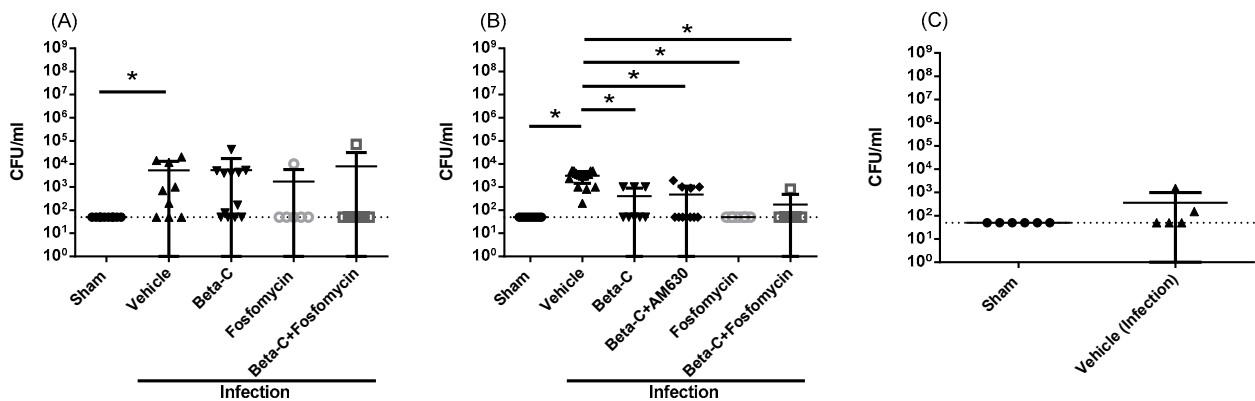


Figure 1. Bacterial burden in the urine of mice (A) 6 hours post inoculation, (B) 24 h post inoculation, and (C) 72 h post inoculation. Animals at the 6 h timepoint were pre-treated at T = 0, while animals at the 24 h timepoint were treated at T = 6 h post inoculation. The dotted line represents the limit of detection (LOD) for the culture method in colony-forming units (CFU) per milliliter (50 CFU/mL). Data presented as mean \pm SD, * $p < 0.05$.

Adhesion and invasion into bladder epithelial cells represent critical points in UTI pathogenesis. We detected low levels of bacterial burden within bladder tissues after 24 h, suggesting some intracellular infiltration occurs at this timepoint (Figure 2A). Treatment with either beta-C or low dose fosfomycin resulted in a significant reduction in tissue bacterial burden, below the limit of detection of the enumeration method. This effect persisted with the administration of AM630. The low levels of infection within tissues are supported by the limited tissue damage observed via histological staining (Supplementary Figure S1E). Immune cells were primarily localized to blood vessels in sham animals (Supplementary Figure S1A,B), with some localized infiltration in infected animals (Supplementary Figure S1C,D).

Following successful bladder infection, UTIs may progress into other tissues. Preliminary data indicates that infection spreads sporadically into the kidney and spleen six hours post inoculation but does not progress to systemic infection of the blood (Figure 2B–D). The bacterial load seen at this early timepoint within some kidneys and spleens appears to resolve spontaneously by the 24 h timepoint (Figure 2B,C), suggesting that the infection generally remains localized to the lower urinary tract. Blood remained sterile at all timepoints (Figure 2D). Levels of pro-inflammatory cytokines within the plasma six hours post inoculation are also indicative of localized infection (Supplementary Figure S2). Within the tissue, elevated IL-6 was observed (Supplementary Figure S2A).

As UTIs frequently result in painful symptoms that persist beyond the administration of antibiotic therapy, we also evaluated the analgesic effects of beta-C treatment. After UTI induction, the animals exhibited significantly increased signs of non-evoked pain, as measured by behavioral scoring (Supplemental Table S1). Behavioral changes persisted from 6 to 24 h post induction and were significantly reduced by treatment with beta-C, both alone and in combination with fosfomycin (Figure 3A,B). In addition, signs of non-evoked pain persisted at 72 h post induction, despite the limited urinary bacterial burden observed (Figure 3C). The administration of the antagonist AM630 did not block the anti-nociceptive effects of the beta-C treatment (Figure 3B). We also evaluated the animals' responsiveness to evoked pain via von Frey esthesiometry (Supplementary Figure S3). The

animals exhibited a significant decrease in their tolerance for applied suprapubic pressure at the 24 h timepoint which did not resolve with beta-C treatment alone (Supplementary Figure S3B). Treatment with beta-C in combination with AM630 significantly reduced this response. No significant changes in pain response were observed at either 6 or 72 h post infection (Supplementary Figure S3A,C).

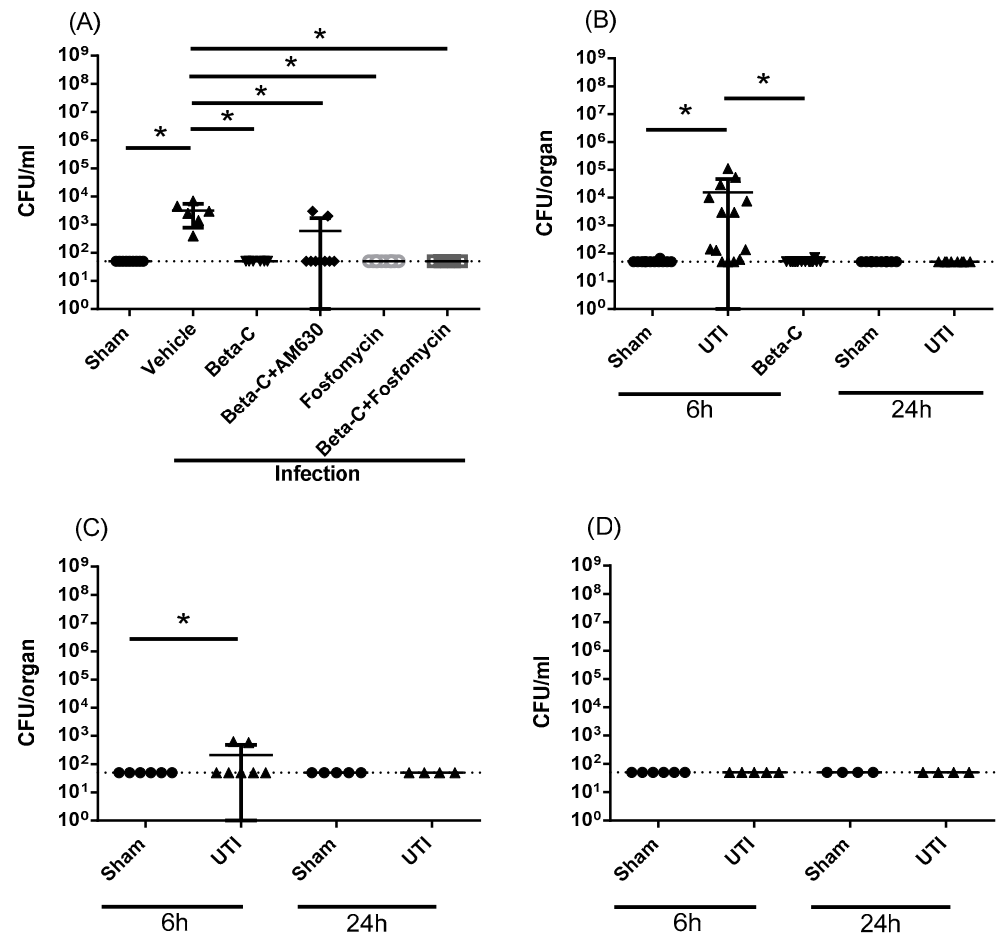


Figure 2. Infection parameters as assessed in mice 6, 24 and 72 h post induction of UTI. Animals at the 6 h timepoint were pre-treated at T = 0, while animals at the 24 h timepoint were treated at T = 6 h post inoculation. Bacterial burden was assessed in the bladder at 24 h (A), and within the kidneys at 6 and 24 h (B). Systematic parameters were also assessed, including spread to spleen (C) and blood (D) at 6 and 24 h. Data presented as mean \pm SD, * $p < 0.05$.

Using IVM, we investigated the effect of beta-C treatment on inflammatory changes within the bladder microvasculature. Adherent leukocytes within venules of an infected bladder are shown in Figure 4D. We observed a significant increase in both rolling and adherent leukocytes 24 h after UTI induction, representing an increase in leukocyte activation (Figure 4A,B). Treatment with beta-C reduced levels of adherent but not rolling leukocytes. AM630 administration did not prevent the observed reduction in adherent leukocytes (Figure 4B). Fosfomycin treatment also resulted in a significant decrease in adherent leukocytes. We also assessed FCD as a marker of changes in microvascular function related to inflammation. UTI induction resulted in a significant decrease in FCD, which was restored with beta-C treatment (Figure 3C). AM630 administration partially reduced the effect of beta-C treatment on FCD.

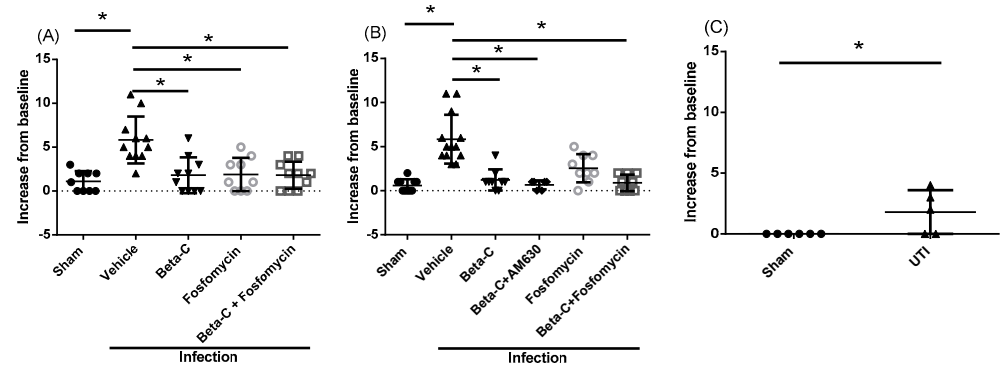


Figure 3. Behavioral changes in infected mice. Changes in behavioral score are shown for mice (A) 6 h, (B) 24 h, and (C) 72 h post inoculation. Animals at the 6 h timepoint were pre-treated at T = 0, while animals at the 24 and 72 h timepoints were treated at T = 6 h post inoculation. Data presented as mean \pm SD, * $p < 0.05$.

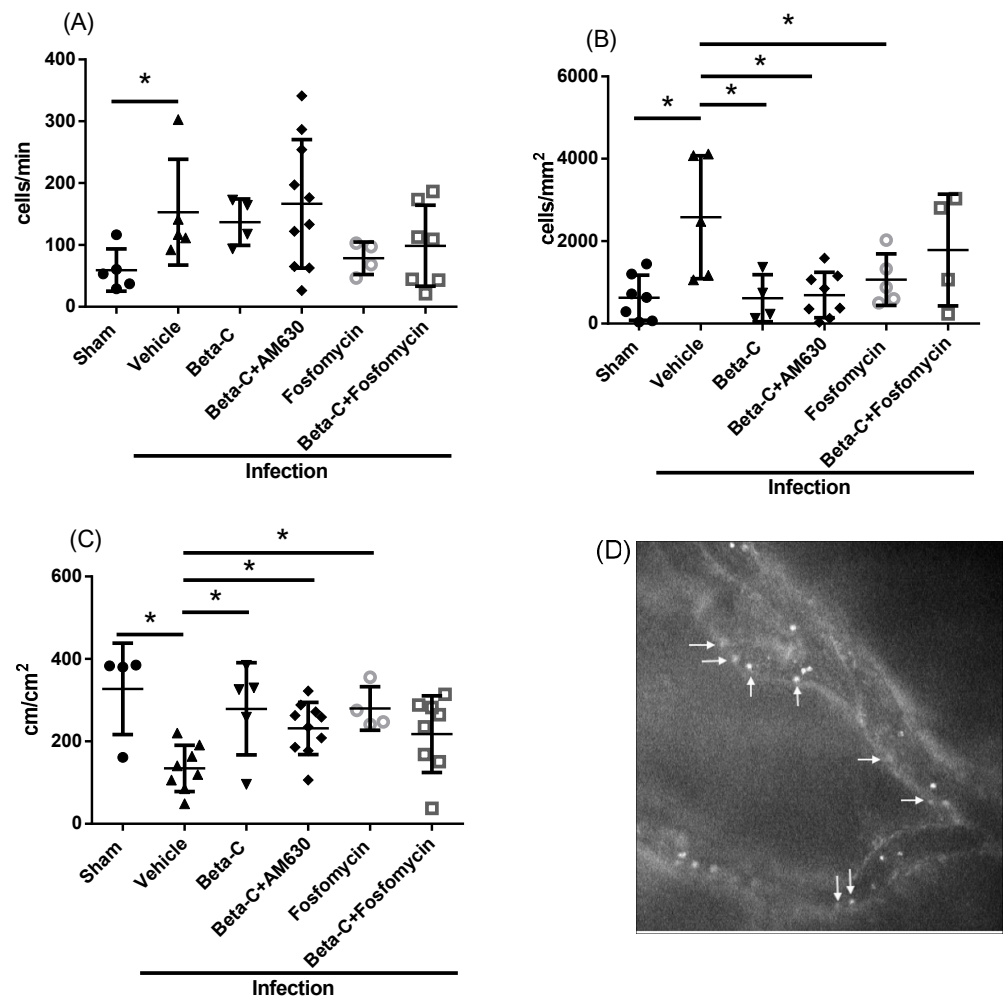


Figure 4. Changes in the bladder microcirculation as assessed in mice 24 h after the induction of a UTI. Using IVM, levels of rolling (A) and adhering (B) leukocytes were assessed. Functional capillary density (FCD; (C)) was also evaluated. Animals were treated at T = 6 h post inoculation and underwent IVM at T = 24 h. Adherent leukocytes are shown within the bladder venules at a magnification of 200 \times (D), as indicated by white arrows. Data presented as mean \pm SD, * $p < 0.05$.

3. Discussion

The primary goal of this study was to evaluate the sesquiterpene beta-C for the management of UTIs, both alone and in combination with antibiotic treatment. While UTIs are generally treatable with standard antibiotic therapies, these therapies do not adequately manage pain or inflammation, can have unpleasant side effects, and may have limited efficacy against antibiotic-resistant pathogens. Based on the anti-inflammatory and anti-nociceptive profile of beta-C and the emerging data suggesting anti-bacterial activity, we hypothesized that beta-C administration would be a promising approach for the management of UTIs.

We first sought to evaluate the anti-bacterial effects of beta-C in a murine model of UTI. The intravesical administration of UPEC resulted in UTI which persisted from 6 to 24 h and resulted in limited systemic spread. Using an optimized timepoint of 24 h, we identified anti-bacterial effects in both the urine and bladder tissues of female BALB/c mice. A significant reduction in the bacterial burden was observed in both the urine and bladder tissues, suggesting that beta-C has anti-bacterial effects in this setting. Several studies have previously demonstrated similar effects in vitro. Dahham et al. demonstrated anti-bacterial activity against six bacterial strains, including *E. coli* [24]. Similarly, Neta et al. demonstrated anti-bacterial activity against *E. coli* in infected murine hepatoma cells [25]. Several other studies have also shown anti-bacterial effects against a variety of pathogens, but the mechanism of activity is yet to be described [26,27]. Importantly, we observed no significant differences in either urinary or bladder tissue bacterial burden between treatment with either beta-C or low-dose fosfomycin, which suggests beta-C may have similar anti-bacterial efficacy to fosfomycin at the selected dosage.

We next sought to evaluate the anti-nociceptive effects of beta-C in our model of murine UTI. We observed a significant increase in signs of non-evoked pain 6 h post-inoculation, which persisted from 24 to 72 h. Significant evoked pain responses were only observed at the 24 h timepoint. The pain levels were highly variable despite the exclusion of mice without robust infections at the 24 and 72 h timepoints. A similar study by Rudick et al. determined that there was no correlation between pelvic pain and bladder colonization, but there are no data available with respect to non-evoked pain [28]. Beta-C treatment, either alone or in combination with fosfomycin, was able to significantly reduce the levels of non-evoked pain at both the 6 and 24 h timepoints. The administration of CB₂R antagonist AM630 did not abrogate this effect, which is likely attributable to the local anesthetic effects associated with the beta-C treatment [23].

Although UTIs are frequently associated with painful symptoms, the mechanisms responsible remain unclear. This is illustrated by the lack of painful symptoms present in cases of asymptomatic bacteriuria, defined as the presence of more than 10⁵ CFU/mL within the urine without typical symptoms of infection [29]. A recent study by Rosen and Klumpp suggests that early pain responses are related to interactions between LPS and TLR4 and may be separated from inflammatory pathways [30]. The authors further determined that TRPV1 and the MCP-1/CCR2 axis are involved [31]. These findings suggest that the majority of UTI pain is mediated by receptors other than CB₂R and may explain the variable responses to beta-C treatment that we observed in this study. There is currently no consensus regarding the effects of beta-C on TRPV1, but evidence suggests that beta-C inhibits MCP-1 secretion [32–34]. This suggests beta-C may also represent a valuable strategy for managing pain associated with either TRPV1 or the MCP-1/CCR2 axis.

The onset of UTI is associated with a significant inflammatory response, characterized by the production of pro-inflammatory mediators by both urothelial cells and immune cells. Major cytokines produced during UTI include TNF- α , IL-1 β , IL-6, IL-8, and IFN- γ [35]. We did not observe significant increases in tissue levels of the majority of cytokines investigated at either the 6 h or 24 h timepoints. This may be related to the attenuation of the immune response by the UPEC strain CFT073, which interferes with both TLRs and the NLRP3 inflammasome via the expression of Toll/IL-1-receptor-containing

protein C (TpcC) [36,37]. A significant but low level of IL-6 was observed at the early timepoint, which correlates with the partial suppression observed by Yadav et al. [38].

Despite relatively low levels of cytokine expression, including neutrophil chemoattractant CXCL2, we observed a significant influx of leukocytes into the bladder microvasculature, with IVM showing significant increases in the number of both rolling and adherent leukocytes. Previous studies have also shown the rapid recruitment of neutrophils into inflamed bladder tissue, with levels peaking 24 h post infection [39,40]. Treatment with beta-C resulted in a significant decrease in the number of adherent leukocytes, which aligns with our previous study investigating the anti-inflammatory effects of beta-C in a sterile model of bladder inflammation [17]. CB₂R activation has also had similar effects in other inflamed tissues, such as the retina, brain, and small intestine [41–43]. These effects could be reversed by the administration of the pharmacological CB₂R antagonist AM630, which contrasts with what we observed in our study. Levels of rolling leukocytes were unaffected by beta-C treatment, either alone or in combination with AM630. Other studies have shown mixed results with respect to the effects of CB₂R activation on leukocyte rolling, indicating that more research is needed to fully understand the effects of beta-C in this context [44–46]. Importantly, beta-C treatment had similar anti-inflammatory effects when compared to fosfomycin therapy alone, which is known to exert some immunosuppressive effects on leukocytes [47].

Microcirculatory changes in response to inflammation have been described in the bladder, including a reduction in functionally perfused capillaries and decreased red blood cell velocity [17,48]. To our knowledge, this is the first study to describe these changes in the context of UTI. We observed a significant decrease in FCD 24 h post UTI induction, which was restored to baseline levels with beta-C treatment. This mirrors findings seen in a sterile model of bladder inflammation in which CB₂R activation by either beta-C or agonist HU-308 resulted in significant improvements in FCD [17]. Notably, CB₂R receptor blockade with AM630 did not completely abrogate the improvements in capillary perfusion seen with beta-C treatment. While this finding suggests some role for CB₂R activation in the modulation of microcirculatory perfusion, it also suggests the involvement of other pathways. A wide variety of factors are known to affect microcirculatory perfusion, including altered blood flow regulation, changes in capillary permeability, and the activation of the coagulation cascade [49,50]. As none of our treatments were able to fully restore microvascular perfusion during UTI regardless of reductions in the bacterial burden/inflammation, more research into the mechanisms at play is merited.

4. Materials and Methods

4.1. Bacterial Strain and Culture Conditions

The uropathogenic *Escherichia coli* (UPEC) strain CFT073 (American Type Culture Collection 700928, Cedar Lane, Burlington, ON, Canada), isolated from a female pyelonephritis patient, was used in this study [51]. Rifampicin resistance was induced via repeated subculturing in sublethal concentrations of rifampicin as previously described [52]. Bacteria were routinely grown on nutrient agar plates at 37 °C with rifampicin as required (50 µg/mL in dimethyl sulfoxide). Prior to infection, UPEC were grown overnight in nutrient broth (with shaking at 37 °C), and then subcultured into fresh broth to encourage the expression of type 1 fimbriae.

4.2. Murine Model of Lower UTI

Female BALB/C mice (8–12 weeks old, 18–25 g) were purchased from Charles River Laboratories International Inc. (Wilmington, MS, USA) and housed in ventilated cage racks at the Carleton Animal Care Facility, Faculty of Medicine, Dalhousie University, Halifax, NS, Canada. The animals were provided with a standard diet of rodent chow with water access ad libitum and kept on a 12 h light/dark cycle. All experimental protocols were performed following the guidelines set forth by the Canadian Council on Animal Care and approved by the Dalhousie University Committee on Laboratory Animals.

The mouse infection studies were performed as previously described by Hannan and Hunstad, with some modifications [53]. In brief, the animals were anesthetized using isoflurane, and the bladder was manually voided. A sterile catheter (P10 polyethylene tubing) was inserted transurethrally, and 50 μ L of UPEC ($1\text{--}2 \times 10^8$ CFU/mL in D-PBS) was slowly instilled into the bladder to minimize the chance of vesicoureteral reflux. The animals received intraperitoneal injections of beta-caryophyllene ($\geq 80\%$, $\leq 19\%$ C15H24 hydrocarbons, Sigma-Aldrich, St. Louis, MO, USA; 100 mg/kg, 20 mg/mL in an olive oil vehicle), fosfomycin (Verity Pharmaceuticals, Mississauga, ON, Canada; 10 mg/kg, 33.3 mg/mL in saline) or a combination therapy of beta-C and fosfomycin. Beta-C doses were based on in vivo toxicity studies which indicated that the lethal dose in murine models exceeds 2000 mg/kg [54]. For preliminary studies, the animals were treated immediately following the induction of UTI and then evaluated after six hours. To enhance clinical relevance, the animals in extended timepoints received treatment 6 h after induction and were then evaluated after either 24 or 72 h post-induction. For extended timepoints, animals were excluded from the analysis if the urinary bacterial burden fell below 10^3 CFU/mL. All animals were humanely sacrificed using approved protocols.

Antagonist studies were conducted at the 24 h timepoint to determine the effects of a CB₂R antagonist on the efficacy of beta-C treatment. AM630 (Millipore Sigma, Burlington, MA, USA; 2.5 mg/kg) was administered via intraperitoneal injection 30 min prior to beta-C treatment. Mice were evaluated as previously described 24 h post induction.

4.3. Pain and Behavior Assessment

Electronic von Frey esthesiometry (IITC Inc. Life Science 2390 series, Woodland Hills, CA, USA) was performed to assess changes in pain tolerance. The suprapubic region was probed to measure the amount of force tolerated (in grams) before the animal reacted (e.g., withdrawal). Prior to assessment, animals were acclimatized to the von Frey apparatus on each of the two days prior to experimentation. Prior to UTI induction, the animals were allowed to acclimate in the quiet, dim procedure room for one hour prior to assessment. The animals were then moved to a plexiglass enclosure with a mesh floor (IITC Life Sciences, Woodland Hills, CA, USA) and allowed to acclimatize for 15 min in the presence of the observer. The esthesiometer, with the rigid tip attached, was slowly applied to the suprapubic region until withdrawal occurred. Five values were recorded, allowing at least 30 s between measurements, forming a baseline for pain tolerance. This procedure was repeated at either 6, 24 or 72 h post UTI induction.

Changes in behavior were assessed using a behavioral scoring system adapted from Boucher et al. [55]. A baseline score was recorded prior to the von Frey assessment and UTI induction. Posture, motor activity, and eye opening were assessed on a scale of 1–10 for a maximum score of 30. Full assessment criteria are available in the supplemental material (Supplementary Table S1). This procedure was repeated at either 6, 24 or 72 h post UTI induction.

4.4. Intravital Microscopy

Intravital microscopy (IVM) of the bladder was used to assess changes in immune activation, as evidenced by leukocyte rolling and adhesion and changes in the capillary perfusion of the bladder wall. IVM was performed 24 h after UTI induction using an epifluorescent microscope (Leica, DM LM, Wetzlar, Germany), set to $20\times$ magnification, and a light source (LEG EBQ 100, Jena, Germany). Briefly, the animals were anesthetized to surgical depth with sodium pentobarbital (65 mg/kg; Ceva Sante Animale, Montreal, QC, Canada) and maintained with repeated administration of 5 mg/kg sodium pentobarbital. Just prior to IVM, the animals were injected via the tail vein with Rhodamine 6G (1.5 mL/kg, 0.75 mg/kg body weight, Sigma-Aldrich, Oakville, ON, Canada) and fluorescein isothiocyanate (FITC)-albumin (1 mL/kg, 50 mg/kg, Sigma-Aldrich, Oakville, ON, Canada). Rhodamine 6G allows for the visualization of leukocytes, while FITC-albumin is used to visualize functional capillary density by illuminating the capillary beds of the

bladder. The bladder was inflated with sterile saline to improve visualization. Leukocytes were visualized using green light, and six to eight visual fields containing bladder venules were randomly selected and recorded for 30 s. Capillary blood flow was then examined using FITC-albumin under blue light. Again, six to eight randomly selected visual fields with capillaries were recorded for 30 s.

4.5. Bacterial Enumeration

Tissue and fluid samples were collected at the experimental endpoint to quantify the bacterial burden in various organs. Urine and plasma were collected, serially diluted, and plated onto nutrient agar plates containing rifampicin. Tissues (bladder, kidneys, and spleen) were aseptically removed and homogenized prior to serial dilution and plating. Plates were incubated at 37 °C, and colony-forming units were counted after 16–24 h.

4.6. Analysis of Bladder Tissue Cytokines

Bladder tissue samples were collected at the experimental endpoint for cytokine analysis. The bladder was bisected along the transverse plane, and the upper dome of the bladder was flash frozen in liquid nitrogen and then stored at −80 °C. Protein concentration was determined via bicinchoninic acid assay (BCA), according to the manufacturer's instructions (Rapid Gold BCA, Protein Assay, Thermo Fisher Scientific, Waltham, MA, USA). A custom-designed mouse cytokine 10-plex kit (R&D Systems, Minneapolis, MN, USA) was used to determine the concentrations of the following cytokines in tissue homogenates: intercellular adhesion molecule 1 (ICAM-1), interleukin 1 (IL-1), interleukin 10 (IL-10), interleukin-6 (IL-6), chemokine CXC ligand 1 (CXCL1), chemokine CXC ligand 2 (CXCL2), P-selectin, interferon-gamma (IFN- γ), LIX recombinant mouse CXC motif chemokine 5 (LIX), and tumor necrosis factor alpha (TNF- α). Samples were prepared according to the manufacturer's protocol and read using a Bio-Plex 200 Analyzer with Bio-Plex Manager software (Bio-Rad, Mississauga, ON, Canada).

4.7. Bladder Histopathology

The lower portion of the bisected bladder was fixed in 10% neutral buffered formalin and then stored in 70% ethanol prior to processing to prevent the overfixation of tissues. Tissue samples were processed and embedded in paraffin, and then 5 μ m sections were cut and transferred onto glass slides for staining. The samples were stained using a standard protocol for hematoxylin and eosin stain (H&E). The bladder samples were scored using a bladder inflammation grading scale adapted from Hopkins et al. [56]. In brief, the tissues were evaluated based on the presence and localization of immune cells and tissue edema/necrosis.

4.8. Statistical Analysis

Data are expressed as the mean \pm standard deviation (SD). Statistical analyses were conducted using GraphPad Prism 6.0 (GraphPad Software Inc., La Jolla, CA, USA). The data were evaluated for normality using the Kolmogorov–Smirnov test, and outliers were removed using Tukey's method. Parametric data were then assessed via a one-way ANOVA with Tukey's multiple comparisons test. Non-parametric data were assessed using the Kruskal–Wallis test with Dunn's multiple comparisons test. Differences of $p < 0.05$ were considered statistically significant.

5. Conclusions

Our study investigated the effects of CB₂R agonist beta-C on infection, pain, and inflammation during UTI. Beta-C treatment resulted in a significant reduction in bacterial burden within both the urine and the bladder tissue 24 h post infection. We also observed a significant reduction in markers of pain and inflammation, including behavioral scoring, leukocyte adhesion, and FCD. Further research is needed to fully understand the effects of beta-C in the context of UTI, including the mechanisms of both anti-bacterial and anti-

nociceptive effects. These results provide evidence supporting the utility of beta-C as a new adjunct therapy for the management of UTIs.

Supplementary Materials: The following supporting information can be downloaded at: <https://www.mdpi.com/article/10.3390/molecules28104144/s1>, Table S1. Murine behavioral scoring parameters; Figure S1. Representative histology images show features of inflammation. Panel (A,B) show a representative score of 0 taken from a sham (uninfected) animal, with blood-vessel-confined immune cells (A; 400×). Cells were identified to be primarily neutrophils (B; 1000×). Panel (C,D) show a bladder sample (score = 0.75) from a UPEC-infected mouse, with focal collections of immune cells further away from the blood vessels (C). Cells were primarily neutrophils and lymphocytes (D). Tissue damage scores, as assessed by hematoxylin and eosin staining of the bladder tissue of mice 6 and 24 h post induction of UTI (E). Data presented as mean ± SD, * $p < 0.05$; Figure S2. Changes in cytokine levels in the bladder tissue, measured via multiplex cytokine assay, as assessed in mice 6 and 24 h post induction of UTI. Cytokines measured included IL-6 (A; undetectable at 24 h), CXCL2 (B; undetectable at 24 h), P-selectin (C), I-CAM-1 (D), IL-10 (E), and LIX (F). Data presented as mean ± SD, * $p < 0.05$; Figure S3. Changes in the evoked pain threshold, measured via von Frey esthesiometry, as assessed in mice 6 (A), 24 (B), and 72 h (C) post induction of UTI. Data presented as mean ± SD, * $p < 0.05$.

Author Contributions: Conceptualization, K.D., C.S., J.Z., M.K. and C.L.; data curation, K.D. and C.S.; formal analysis, K.D., C.S. and C.L.; funding acquisition, J.Z., M.K. and C.L.; investigation, K.D., C.S. and H.W.; methodology, K.D., C.S. and C.L.; resources, J.Z., M.K. and C.L.; supervision, J.Z., M.K. and C.L.; validation, K.D., C.S. and H.W.; visualization, K.D.; writing—original draft, K.D., C.S. and H.W.; writing—review and editing, K.D., C.S., H.W. and C.L. All authors have read and agreed to the published version of the manuscript.

Funding: This research was funded by MITACS Canada (IT5647).

Institutional Review Board Statement: The animal study protocol was approved by the Dalhousie University Committee on Laboratory Animals (protocol code 21-032 and date of approval).

Data Availability Statement: Not applicable.

Acknowledgments: The authors acknowledge the support of Tanya Myers, Bithika Ray, and Cheng Wang.

Conflicts of Interest: The authors declare no conflict of interest.

Sample Availability: Samples of the compounds are not available from the authors.

References

1. Flores-Mireles, A.L.; Walker, J.N.; Caparon, M.; Hultgren, S.J. Urinary Tract Infections: Epidemiology, Mechanisms of Infection and Treatment Options. *Nat. Rev. Microbiol.* **2015**, *13*, 269–284. [[CrossRef](#)] [[PubMed](#)]
2. Zeng, Z.; Zhan, J.; Zhang, K.; Chen, H.; Cheng, S. Global, Regional, and National Burden of Urinary Tract Infections from 1990 to 2019: An Analysis of the Global Burden of Disease Study 2019. *World J. Urol.* **2022**, *40*, 755–763. [[CrossRef](#)] [[PubMed](#)]
3. Foxman, B. The Epidemiology of Urinary Tract Infection. *Nat. Rev. Urol.* **2010**, *7*, 653–660. [[CrossRef](#)] [[PubMed](#)]
4. Glover, M.; Moreira, C.G.; Sperandio, V.; Zimmern, P. Recurrent Urinary Tract Infections in Healthy and Nonpregnant Women. *Urol. Sci.* **2014**, *25*, 1–8. [[CrossRef](#)] [[PubMed](#)]
5. Gupta, K.; Hooton, T.M.; Naber, K.G.; Wullt, B.; Colgan, R.; Miller, L.G.; Moran, G.J.; Nicolle, L.E.; Raz, R.; Schaeffer, A.J.; et al. International Clinical Practice Guidelines for the Treatment of Acute Uncomplicated Cystitis and Pyelonephritis in Women: A 2010 Update by the Infectious Diseases Society of America and the European Society for Microbiology and Infectious Diseases. *Clin. Infect. Dis.* **2011**, *52*, 103–120. [[CrossRef](#)]
6. Ganguly, N.; Giang, P.H.; Gupta, C.; Basu, S.K.; Siddiqui, I.; Salunke, D.M.; Sharma, P. Mycobacterium Tuberculosis Secretory Proteins CFP-10, ESAT-6 and the CFP10:ESAT6 Complex Inhibit Lipopolysaccharide-Induced NF-KB Transactivation by Downregulation of Reactive Oxidative Species (ROS) Production. *Immunol. Cell Biol.* **2008**, *86*, 98–106. [[CrossRef](#)]
7. Brown, P.D. Impact of Changing Patterns of Anti-Microbial Resistance in Uropathogens: Emerging Treatment and Strategies. *Curr. Infect. Dis. Rep.* **2003**, *5*, 499–503. [[CrossRef](#)]
8. DeMarsh, M.; Bookstaver, P.B.; Gordon, C.; Lim, J.; Griffith, N.; Bookstaver, N.K.; Justo, J.A.; Kohn, J.; Al-Hasan, M.N. Prediction of Trimethoprim/Sulfamethoxazole Resistance in Community-Onset Urinary Tract Infections. *J. Glob. Antimicrob. Resist.* **2020**, *21*, 218–222. [[CrossRef](#)]

9. Gardiner, B.J.; Stewardson, A.J.; Abbott, I.J.; Peleg, A.Y. Nitrofurantoin and Fosfomycin for Resistant Urinary Tract Infections: Old Drugs for Emerging Problems. *Aust. Prescr.* **2019**, *42*, 14–19. [[CrossRef](#)]
10. Critchley, I.A.; Cotroneo, N.; Pucci, M.J.; Mendes, R. The Burden of Antimicrobial Resistance among Urinary Tract Isolates of *Escherichia coli* in the United States in 2017. *PLoS ONE* **2019**, *14*, e0220265. [[CrossRef](#)]
11. Mohsen, S.; Dickinson, J.A.; Somayaji, R. Update on the Adverse Effects of Antimicrobial Therapies in Community Practice. *Can. Fam. Physician* **2020**, *66*, 651–659. [[PubMed](#)]
12. Colgan, R.; Williams, M. Diagnosis and Treatment of Acute Uncomplicated Cystitis. *Am. Fam. Physician* **2011**, *84*, 771–776. [[PubMed](#)]
13. Pertwee, R.G. The Therapeutic Potential of Drugs That Target Cannabinoid Receptors or Modulate the Tissue Levels or Actions of Endocannabinoids. *Drug Addict. From Basic Res. Ther.* **2008**, *7*, 637–686. [[CrossRef](#)]
14. Zou, S.; Kumar, U. Cannabinoid Receptors and the Endocannabinoid System: Signaling and Function in the Central Nervous System. *Int. J. Mol. Sci.* **2018**, *19*, 833. [[CrossRef](#)]
15. Merriam, F.V.; Wang, Z.; Guerios, S.D.; Bjorling, D.E. Cannabinoid Receptor 2 Is Increased in Acutely and Chronically Inflamed Bladder of Rats. *Neurosci. Lett.* **2008**, *445*, 130–134. [[CrossRef](#)]
16. Christie, S.; Brookes, S.; Zagorodnyuk, V. Endocannabinoids in Bladder Sensory Mechanisms in Health and Diseases. *Front. Pharmacol.* **2021**, *12*, 708989. [[CrossRef](#)]
17. Berger, G.; Arora, N.; Burkovskiy, I.; Xia, Y.; Chinnadurai, A.; Westhofen, R.; Hagn, G.; Cox, A.; Kelly, M.; Zhou, J.; et al. Experimental Cannabinoid 2 Receptor Activation by Phyto-Derived and Synthetic Cannabinoid Ligands in LPS-Induced Interstitial Cystitis in Mice. *Molecules* **2019**, *24*, 4239. [[CrossRef](#)]
18. Gertsch, J.; Leonti, M.; Raduner, S.; Racz, I.; Chen, J.Z.; Xie, X.Q.; Altmann, K.H.; Karsak, M.; Zimmer, A. Beta-Caryophyllene Is a Dietary Cannabinoid. *Proc. Natl. Acad. Sci. USA* **2008**, *105*, 9099–9104. [[CrossRef](#)]
19. Maffei, M.E. Plant Natural Sources of the Endocannabinoid (E)- β -Caryophyllene: A Systematic Quantitative Analysis of Published Literature. *Int. J. Mol. Sci.* **2020**, *21*, 6540. [[CrossRef](#)]
20. Smedman, L.Å.; Snajberk, K.; Zavarin, E.; Mon, T.R. Oxygenated Monoterpenoids and Sesquiterpenoid Hydrocarbons of the Cortical Turpentine from Different *Abies* Species. *Phytochemistry* **1969**, *8*, 1471–1479. [[CrossRef](#)]
21. Bastaki, M.; Api, A.M.; Aubanel, M.; Bauter, M.; Cachet, T.; Demyttenaere, J.C.R.; Diop, M.M.; Harman, C.L.; Hayashi, S.M.; Krammer, G.; et al. Dietary Administration of β -Caryophyllene and Its Epoxide to Sprague-Dawley Rats for 90 Days. *Food Chem. Toxicol.* **2020**, *135*, 110876. [[CrossRef](#)]
22. Klauke, A.-L.; Racz, I.; Pradier, B.; Markert, A.; Zimmer, A.M.; Gertsch, J.; Zimmer, A. The Cannabinoid CB2 Receptor-Selective Phytocannabinoid Beta-Caryophyllene Exerts Analgesic Effects in Mouse Models of Inflammatory and Neuropathic Pain. *Eur. Neuropsychopharmacol.* **2014**, *24*, 608–620. [[CrossRef](#)] [[PubMed](#)]
23. Ghelardini, C.; Galeotti, N.; Di Cesare Mannelli, L.; Mazzanti, G.; Bartolini, A. Local Anaesthetic Activity of β -Caryophyllene. *Farmaco* **2001**, *56*, 387–389. [[CrossRef](#)]
24. Neta, M.C.S.; Vittorazzi, C.; Guimarães, A.C.; Martins, J.D.L.; Fronza, M.; Endringer, D.C.; Scherer, R. Effects of β -Caryophyllene and *Murraya paniculata* Essential Oil in the Murine Hepatoma Cells and in the Bacteria and Fungi 24-h Time-Kill Curve Studies. *Pharm. Biol.* **2017**, *55*, 190–197. [[CrossRef](#)] [[PubMed](#)]
25. Yoo, H.J.; Jwa, S.K. Inhibitory Effects of β -Caryophyllene on Streptococcus Mutans Biofilm. *Arch. Oral Biol.* **2018**, *88*, 42–46. [[CrossRef](#)]
26. Dahham, S.S.; Tabana, Y.M.; Iqbal, M.A.; Ahamed, M.B.K.; Ezzat, M.O.; Majid, A.S.A.; Majid, A.M.S.A. The Anticancer, Antioxidant and Antimicrobial Properties of the Sesquiterpene β -Caryophyllene from the Essential Oil of *Aquilaria crassna*. *Molecules* **2015**, *20*, 11808–11829. [[CrossRef](#)]
27. Pieri, F.A.; Souza, M.C.d.C.; Vermelho, L.L.R.; Vermelho, M.L.R.; Perciano, P.G.; Vargas, F.S.; Borges, A.P.B.; da Veiga-Junior, V.F.; Moreira, M.A.S. Use of β -Caryophyllene to Combat Bacterial Dental Plaque Formation in Dogs. *BMC Vet. Res.* **2016**, *12*, 216. [[CrossRef](#)] [[PubMed](#)]
28. Rudick, C.N.; Billips, B.K.; Pavlov, V.I.; Yaggie, R.E.; Schaeffer, A.J.; Klumpp, D.J. Host-Pathogen Interactions Mediating Pain of Urinary Tract Infection. *J. Infect. Dis.* **2010**, *201*, 1240–1249. [[CrossRef](#)]
29. Owens, D.K.; Davidson, K.W.; Krist, A.H.; Barry, M.J.; Cabana, M.; Caughey, A.B.; Doubeni, C.A.; Epling, J.W.; Kubik, M.; Landefeld, C.S.; et al. Screening for Asymptomatic Bacteriuria in Adults: US Preventive Services Task Force Recommendation Statement. *JAMA-J. Am. Med. Assoc.* **2019**, *322*, 1188–1194. [[CrossRef](#)]
30. Rosen, J.M.; Klumpp, D.J. Mechanisms of Pain from Urinary Tract Infection. *Int. J. Urol.* **2014**, *21*, 26–32. [[CrossRef](#)]
31. Rosen, J.M.; Yaggie, R.E.; Woida, P.J.; Miller, R.J.; Schaeffer, A.J.; Klumpp, D.J. TRPV1 and the MCP-1/CCR2 Axis Modulate Post-UTI Chronic Pain. *Sci. Rep.* **2018**, *8*, 7188. [[CrossRef](#)] [[PubMed](#)]
32. Heblinski, M.; Santiago, M.; Fletcher, C.; Stuart, J.; Connor, M.; McGregor, I.S.; Arnold, J.C. Terpenoids Commonly Found in *Cannabis sativa* Do Not Modulate the Actions of Phytocannabinoids or Endocannabinoids on TRPA1 and TRPV1 Channels. *Cannabis Cannabinoid Res.* **2020**, *5*, 305–317. [[CrossRef](#)] [[PubMed](#)]
33. Serra, M.P.; Boi, M.; Carta, A.; Murru, E.; Quartu, M.; Carta, G.; Banni, S. Anti-Inflammatory Effect of Beta-Caryophyllene Mediated by the Involvement of TRPV1, BDNF and TrkB in the Rat Cerebral Cortex after Hypoperfusion/Reperfusion. *Int. J. Mol. Sci.* **2022**, *23*, 3633. [[CrossRef](#)]

34. Jung, J.I.; Kim, E.J.; Kwon, G.T.; Jung, Y.J.; Park, T.; Kim, Y.; Yu, R.; Choi, M.S.; Chun, H.S.; Kwon, S.H.; et al. β -Caryophyllene Potently Inhibits Solid Tumor Growth and Lymph Node Metastasis of B16F10 Melanoma Cells in High-Fat Diet-Induced Obese C57BL/6N Mice. *Carcinogenesis* **2015**, *36*, 1028–1039. [[CrossRef](#)] [[PubMed](#)]
35. Engelsöy, U.; Rangel, I.; Demirel, I. Impact of Proinflammatory Cytokines on the Virulence of Uropathogenic *Escherichia coli*. *Front. Microbiol.* **2019**, *10*, 1051. [[CrossRef](#)]
36. Waldhuber, A.; Puthia, M.; Wieser, A.; Cirl, C.; Dürr, S.; Neumann-Pfeifer, S.; Albrecht, S.; Römmler, F.; Müller, T.; Zheng, Y.; et al. Uropathogenic *Escherichia coli* Strain CFT073 Disrupts NLRP3 Inflammasome Activation. *J. Clin. Investig.* **2016**, *126*, 2425–2436. [[CrossRef](#)]
37. Cirl, C.; Wieser, A.; Yadav, M.; Duerr, S.; Schubert, S.; Fischer, H.; Stappert, D.; Wantia, N.; Rodriguez, N.; Wagner, H.; et al. Subversion of Toll-like Receptor Signaling by a Unique Family of Bacterial Toll/Interleukin-1 Receptor Domain-Containing Proteins. *Nat. Med.* **2008**, *14*, 399–406. [[CrossRef](#)]
38. Yadav, M.; Zhang, J.; Fischer, H.; Huang, W.; Lutay, N.; Cirl, C.; Lum, J.; Miethke, T.; Svanborg, C. Inhibition of TIR Domain Signaling by TcpC: MyD88-Dependent and Independent Effects on *Escherichia coli* Virulence. *PLoS Pathog.* **2010**, *6*, e1001120. [[CrossRef](#)]
39. Schiwon, M.; Weisheit, C.; Franken, L.; Gutweiler, S.; Dixit, A.; Meyer-Schwesinger, C.; Pohl, J.M.; Maurice, N.J.; Thiebes, S.; Lorenz, K.; et al. Crosstalk between Sentinel and Helper Macrophages Permits Neutrophil Migration into Infected Uroepithelium. *Cell* **2014**, *156*, 456–468. [[CrossRef](#)]
40. Zec, K.; Volke, J.; Vijitha, N.; Thiebes, S.; Gunzer, M.; Kurts, C.; Engel, D.R. Neutrophil Migration into the Infected Uroepithelium Is Regulated by the Crosstalk between Resident and Helper Macrophages. *Pathogens* **2016**, *5*, 15. [[CrossRef](#)]
41. Szczesniak, A.M.; Porter, R.F.; Toguri, J.T.; Borowska-Fielding, J.; Gebremeskel, S.; Siwakoti, A.; Johnston, B.; Lehmann, C.; Kelly, M.E.M. Cannabinoid 2 Receptor Is a Novel Anti-Inflammatory Target in Experimental Proliferative Vitreoretinopathy. *Neuropharmacology* **2017**, *113*, 627–638. [[CrossRef](#)] [[PubMed](#)]
42. Lehmann, C.; Kianian, M.; Zhou, J.; Kuster, I.; Kuschnerreit, R.; Whynot, S.; Hung, O.; Shukla, R.; Johnston, B.; Cerny, V.; et al. Cannabinoid Receptor 2 Activation Reduces Intestinal Leukocyte Recruitment and Systemic Inflammatory Mediator Release in Acute Experimental Sepsis. *Crit. Care* **2012**, *16*, R47. [[CrossRef](#)] [[PubMed](#)]
43. Ramirez, S.H.; Haskó, J.; Skuba, A.; Fan, S.; Dykstra, H.; McCormick, R.; Reichenbach, N.; Krizbai, I.; Mahadevan, A.; Zhang, M.; et al. Activation of Cannabinoid Receptor 2 Attenuates Leukocyte-Endothelial Cell Interactions and Blood-Brain Barrier Dysfunction under Inflammatory Conditions. *J. Neurosci.* **2012**, *32*, 4004–4016. [[CrossRef](#)] [[PubMed](#)]
44. Sardinha, J.; Kelly, M.E.M.; Zhou, J.; Lehmann, C. Experimental Cannabinoid 2 Receptor-Mediated Immune Modulation in Sepsis. *Mediat. Inflamm.* **2014**, *2014*, 978678. [[CrossRef](#)]
45. Zhang, M.; Martin, B.R.; Adler, M.W.; Razdan, R.K.; Jallo, J.I.; Tuma, R.F. Cannabinoid CB2 Receptor Activation Decreases Cerebral Infarction in a Mouse Focal Ischemia/Reperfusion Model. *J. Cereb. Blood Flow Metab.* **2007**, *27*, 1387–1396. [[CrossRef](#)]
46. Krustev, E.; Reid, A.; McDougall, J.J. Tapping into the Endocannabinoid System to Ameliorate Acute Inflammatory Flares and Associated Pain in Mouse Knee Joints. *Arthritis Res. Ther.* **2014**, *16*, 1–12. [[CrossRef](#)]
47. Zeitlinger, M.; Marsik, C.; Steiner, I.; Sauermann, R.; Seir, K.; Jilma, B.; Wagner, O.; Joukhadar, C. Immunomodulatory Effects of Fosfomycin in an Endotoxin Model in Human Blood. *J. Antimicrob. Chemother.* **2007**, *59*, 219–223. [[CrossRef](#)]
48. Bajory, Z.; Szabó, A.; Király, I.; Pajor, L.; Messmer, K. Involvement of Nitric Oxide in Microcirculatory Reactions after Ischemia-Reperfusion of the Rat Urinary Bladder. *Eur. Surg. Res.* **2008**, *42*, 28–34. [[CrossRef](#)]
49. Ince, C. Hemodynamic Coherence and the Rationale for Monitoring the Microcirculation. *Crit. Care* **2015**, *19* (Suppl. 3), S8. [[CrossRef](#)]
50. Guven, G.; Hilty, M.P.; Ince, C. Microcirculation: Physiology, Pathophysiology, and Clinical Application. *Blood Purif.* **2020**, *49*, 143–150. [[CrossRef](#)]
51. Welch, R.A.; Burland, V.; Plunkett, G.; Redford, P.; Roesch, P.; Rasko, D.; Buckles, E.L.; Liou, S.-R.; Boutin, A.; Hackett, J.; et al. Extensive Mosaic Structure Revealed by the Complete Genome Sequence of Uropathogenic *Escherichia coli*. *Proc. Natl. Acad. Sci. USA* **2002**, *99*, 17020–17024. [[CrossRef](#)] [[PubMed](#)]
52. Dey, R.; Pal, K.K.; Bhatt, D.M.; Chauhan, S.M. Growth Promotion and Yield Enhancement of Peanut (*Arachis hypogaea* L.) by Application of Plant Growth-Promoting Rhizobacteria. *Microbiol. Res.* **2004**, *159*, 371–394. [[CrossRef](#)] [[PubMed](#)]
53. Hannan, T.J.; Hunstad, D.A. A Murine Model for *Escherichia coli* Urinary Tract Infection. *Methods Mol. Biol.* **2016**, *1333*, 159–175. [[CrossRef](#)]
54. Da Silva Oliveira, G.L.; Machado, K.C.; Machado, K.C.; da Silva, A.P.d.S.C.L.; Feitosa, C.M.; de Castro Almeida, F.R. Non-Clinical Toxicity of β -Caryophyllene, a Dietary Cannabinoid: Absence of Adverse Effects in Female Swiss Mice. *Regul. Toxicol. Pharmacol.* **2018**, *92*, 338–346. [[CrossRef](#)] [[PubMed](#)]
55. Boucher, M.; Meen, M.; Codron, J.P.; Coudore, F.; Kemeny, J.L.; Eschaliier, A. Cyclophosphamide-Induced Cystitis in Freely-Moving Conscious Rats: Behavioral Approach to a New Model of Visceral Pain. *J. Urol.* **2000**, *164*, 203–208. [[CrossRef](#)]
56. Hopkins, W.J.; Gendron-Fitzpatrick, A.; Balish, E.; Uehling, D.T. Time Course and Host Responses to *Escherichia coli* Urinary Tract Infection in Genetically Distinct Mouse Strains. *Infect. Immun.* **1998**, *66*, 2798–2802. [[CrossRef](#)]

Disclaimer/Publisher’s Note: The statements, opinions and data contained in all publications are solely those of the individual author(s) and contributor(s) and not of MDPI and/or the editor(s). MDPI and/or the editor(s) disclaim responsibility for any injury to people or property resulting from any ideas, methods, instructions or products referred to in the content.